$$a_5 = d_5 = \frac{1}{s_5} \tag{25}$$

$$e_5 = \left(\frac{1}{s_1} + \frac{1}{s_2}\cos\theta_2 + a_3 + \frac{1}{s_4}\cos\theta_4\right)L \tag{26}$$

L is the projected length of the fractal dipole as indicated in Fig. 3. Here the geometry of the FAE is uniquely determined by the parameters s_1, s_2, s_4, s_5, θ_2, θ_4 and L. These parameters may be encoded into a genetic algorithm (GA) [4 – 6] for the purpose of determining the optimal FAE configuration that will best satisfy a particular set of design requirements.

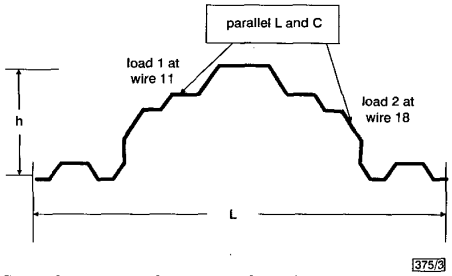

Fig. 3 *General structure of optimised fractal antenna*

GA-FAE design: In this Section we employ a GA approach to evolve an optimal design for a dualband FAE. The target frequencies of the antenna are 1.225 and 1.575 GHz. The VSWR requirements for both frequencies are to be less than 2. In addition to the VSWR requirement, we aim to reduce the size of the antenna by over 50% compared to a conventional half-wave dipole at 1.225 GHz (the lower frequency). Two LC loads were applied to the antenna so that the VSWR requirement can be satisfied at the higher frequency of 1.575 GHz. The genetic algorithm technique was used in conjunction with an IFS fractal generating subroutine and a method of moments (MoM) code to systematically optimise the antenna characteristics, e.g. VSWR and gain. The fractal geometry of the antenna, the load component values (Ls and Cs) and the load locations are the parameters simultaneously optimised by the GA. The GA provides selected parameters, s_1, s_2, s_4, s_5, θ_2, θ_4 and length L, to the fractal generating subroutine that employs the IFS technique to create the FAE geometry. Subsequently, along with the FAE geometry, the LC load component values and the load locations, which are also assigned by the GA, are made available to the MoM code in order to compute the radiation characteristics of the candidate antenna (i.e. VSWR, gain, etc.). Our goal here is to achieve low VSWRs for both of the target frequencies and, therefore, the objective function for the design is chosen to be

$$F = \sum_{i=1}^{N_f} \left|VSWR(f_i) - 1\right|^2 \tag{27}$$

where N_f is the number of frequencies of interest (in this case, they are 1.225 and 1.575 GHz).

Table 1: GA selected parameters and corresponding VSWRs for the three designs

Case	Antenna structure parameters						Load component values				Load location (wire)		Projected length		VSWR	
	S_1	S_2	S_4	S_5	θ_2	θ_4	L_1	L_2	C_1	C_2	Load		L	h	1.225	1.57
					deg		nH		pF		1	2	cm		GHz	GHz
1	5.43	4.83	4.99	5.46	44.29	46.23	15.44	12.05	0.66	0.33	5	25	9	1.75	1.04	1.14
2	5.26	4.74	4.55	5.45	47.36	44.96	19.5	17.95	0.10	0.81	19	23	7	1.49	1.33	1.10
3	5.90	4.70	4.40	5.30	50.44	46.20	12.51	15.87	0.54	0.93	16	22	5.5	1.22	1.94	1.79

Results: Three design examples using the GA-FAE optimisation technique are considered. The general fractal antenna structure for all three cases is illustrated in Fig. 3, which is the second iteration of a generating antenna similar to that shown in Fig. 2. The antenna structure in all three cases consists of 25 wires as illustrated in Fig. 3. The antenna structure parameters, load component values and load locations, which are all selected by the GA, are listed in Table 1 for each of the three designs considered. The first design has a projected length of L = 9 cm and a VSWR of 1.04 and 1.14 for 1.225 and 1.575 GHz, respectively. The second design has a projected length of L = 7 cm and a VSWR of 1.33 and 1.10 for 1.225 and 1.575 GHz, respectively. Finally, the third design has a projected length of only L = 5.5 cm with a corresponding VSWR of 1.94 and 1.79 at 1.225 and 1.575 GHz, respectively. This last case represents an overall size reduction of 55%. Fig. 4*a* shows a conventional half-wave dipole at 1.225 GHz; while Fig. 4*b* shows the geometry of the optimised FAE for the last case. This comparison clearly demonstrates the degree of miniaturisation that can be achieved through the use of the GA-FAE design optimisation technique introduced in the preceding Section.

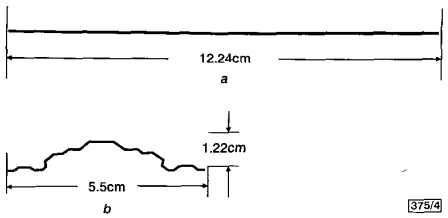

Fig. 4 *Conventional half-wave dipole at 1.225 GHz and geometry of miniaturised fractal dipole for case 3*

a Conventional half-wave dipole
b Geometry of dipole

Conclusion: A genetic algorithm technique has been successfully developed for use in conjunction with an IFS approach for generating fractal geometries and a computational electromagnetics analysis code based on the method of moments to systematically optimise the performance characteristics of FAEs. For the three examples considered, the VSWRs of the optimised FAEs were less than 2 at each of the specified target frequencies. It was also shown that the projected length of a fractal dipole may be reduced by as much as 55% compared to a conventional dipole by the optimal choice of antenna shape as well as load locations and associated component values.

21 June 2001
Electronics Letters Online No: 20010802
DOI: 10.1049/el:20010802

D.H. Werner and P.L. Werner (*Department of Electrical Engineering, The Pennsylvania State University, University Park, PA 16802, USA*)

K.H. Church (*Sciperio, Inc., 5202-2 N. Richmond Hill, Stillwater, OK 74075, USA*)

References

1 PEITGEN, H.-O., JURGENS, H., and SAUPE, D.: 'Chaos and fractals: new frontiers of science' (Springer-Verlag, 1992)
2 BARNSLEY, M.: 'Fractals everywhere' (Academic Press, Inc., 1988)
3 WERNER, D.H., and MITTRA, R.: 'Frontiers in electromagnetics' (IEEE Press, Piscataway, NJ, 2000)
4 HAUPT, R.L., and HAUPT, S.E.: 'Practical genetic algorithms' (John Wiley & Sons, Inc., New York, 1997)
5 RAHMAT-SAMII, Y., and MICHIELSSEN, E.: 'Electromagnetic optimization by genetic algorithms' (John Wiley & Sons, Inc., 1999)
6 COHEN, N.: 'Fractal coding in genetic algorithm (GA) antenna optimisation'. Proc. IEEE Antennas and Propagation Society Int. Symp., Montreal, Canada, July 1997, Vol. 3, pp. 1692–1695

Resonance frequencies of compact microstrip antenna

M. Paulson, S.O. Kundukulam, C.K. Aanandan and P. Mohanan

A simple technique for calculating the resonance frequencies of a compact arrow-shaped microstrip antenna is presented and discussed. The accuracy of the method is validated by experimental results.

Introduction: The arrow shaped microstrip antenna, which produces dual frequency dual polarisation operation with considera-

ble size reduction compared to conventional patches has been reported [1]. These antennas provide greater area reduction and improved gain compared to drum shaped patches [2]. Prediction of the resonance frequency of drum shaped patches [3] and circular patches for broadband operation [4] are available in the literature. In this Letter, we propose empirical formulas for calculating the resonance frequencies of the arrow shaped microstrip antenna. These antennas can be employed for obtaining dual frequency with the same polarisation, bandwidth enhancement, circular polarisation etc. by varying its different parameters or by introducing slots. The proposed design equations provide an easier and simple way of predicting the resonant frequencies of these patches.

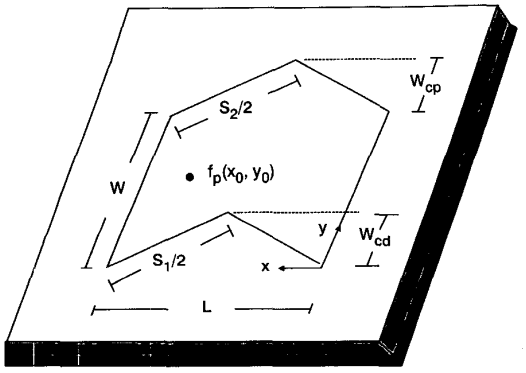

Fig. 1 *Geometry of arrow shaped microstrip antenna*

Frequency calculation: The schematic diagram of the antenna is shown in Fig. 1. The structure consists of an arrow shaped patch with an intruding triangle of height W_{cd} and protruding triangle of height W_{cp} with slanted lengths S_1 and S_2 etched on a dielectric substrate of thickness h and dielectric constant ε_r.

The standard equations for computing the resonant frequency of a rectangular patch antenna are modified to take into account the effect of the intruding and protruding lengths W_{cd} and W_{cp}. The line extension factor and the effective resonating lengths of the two modes are obtained by the following empirical relations:
for the TM_{10} mode

$$f_{10} = \frac{c}{2(S_{eff} + 2\Delta l_1)\sqrt{\varepsilon_1}} \quad (1)$$

$$\varepsilon_1 = \frac{\varepsilon_r + 1}{2} + \frac{\varepsilon_r - 1}{2}(1 + 12h/W)^{-1/2} \quad (2)$$

$$\Delta l_1 = \frac{0.412h(\varepsilon_1 + 0.3)(W/h + 0.258)}{(\varepsilon_1 - 0.258)(W/h + 0.8)} \quad (3)$$

for the TM_{01} mode

$$f_{01} = \frac{c}{2(W_{eff} + 2\Delta l_2)\sqrt{\varepsilon_2}}$$

where ε_2 and Δl_2 are calculated by replacing W by S in eqns. 2 and 3, respectively, with $S = (S_1 + S_2)/2$.

S_{eff} and W_{eff} are calculated as follows:
For ($L < W$)

$$\left.\begin{aligned} S_{eff} &= S_1 - (0.001/L) + 0.01W \\ &\quad - 0.68(W_{cd} - 0.01) - 0.03(W_{cp} - 0.01) \\ W_{eff} &= W + 0.58W_{cp} - 0.43W_{cd} \end{aligned}\right\} \text{for } W_{cd}/W \le 0.5$$

$$\left.\begin{aligned} S_{eff} &= 0.5(S_1 + L) + 0.4W_{cd} \\ &\quad - 0.175W - 0.03(W_{cp} - 0.01) \\ W_{eff} &= 0.78W + 0.025W_{cd} + 0.49W_{cp} \end{aligned}\right\} \text{for } W_{cd}/W > 0.5$$

For ($L >= W$)

$$\begin{aligned} S_{eff} &= S_1 + 2.3(L - 2W - 0.0046/L)W_{cd} \\ &\quad + 0.00006/L - 0.1(W_{cp} - 0.01) && \text{for } W_{cd}/W < 1 \\ W_{eff} &= W + 0.58W_{cp} - 0.43W_{cd} \\ &\quad + 0.0023(L - W)/W && \text{for } W_{cd}/W \le 0.5 \\ W_{eff} &= 0.78W + 0.025W_{cd} + 0.49W_{cp} \\ &\quad + 0.0025W_{cd}/W + 0.17(L - W - 0.01) && \text{for } W_{cd}/W > 0.5 \end{aligned}$$

Comparison of theory and experiment: The theoretical variation of the two resonant frequencies f_{10} and f_{01} with L for different values of W_{cd} and W_{cp} are given in Fig. 2. The experimental curves are also given to validate the computation. To further check the validity, the antennas were fabricated on substrates with different dielectric constants and thickness. The results are shown in Fig. 3. In all these cases the theoretical results are in good agreement with experimental values with maximum error < 2%.

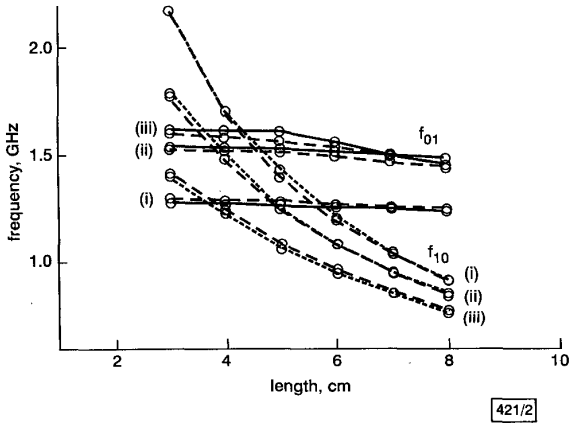

Fig. 2 *Variation of TM_{10} and TM_{01} mode frequencies with length L for different W_{cp} and W_{cd} (W = 5 cm)*

—○— calculated
– –○– – measured
(i) W_{cd} = 1, W_{cp} = 2
(ii) W_{cd} = 2, W_{cp} = 1
(iii) W_{cd} = 3, W_{cp} = 1

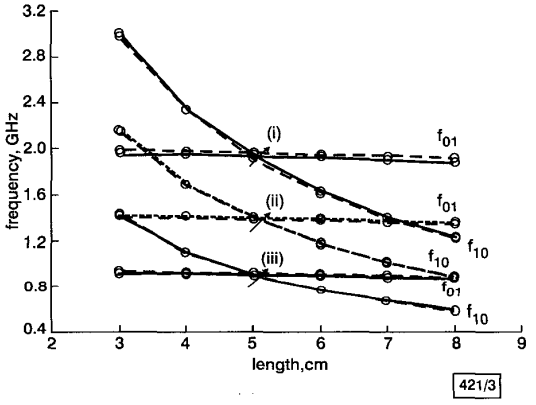

Fig. 3 *Variation of TM_{10} and TM_{01} mode frequencies with length L for different ε_r and h values*

—○— calculated
– –○– – measured
(i) ε_r = 2.2, h = 0.08
(ii) ε_r = 4.28, h = 0.16
(iii) ε_r = 10.2, h = 0.066

Conclusion: A simple and accurate technique to determine the resonance frequencies of the dominant modes of a compact arrow shaped patch antenna is presented. The method is validated by experimental results and the percentage error is found to be < 2%. This method of frequency prediction is less time consuming than the expensive simulation software.

3 July 2001
Electronics Letters Online No: 20010814
DOI: 10.1049/el:20010814

M. Paulson, S.O. Kundukulam, C.K. Aanandan and P. Mohanan (*Centre for Research in Electromagnetics and Antennas, Department of Electronics, Cochin University of Science and Technology, Cochin 682 022, India*)

E-mail: aanandan@doe.cusat.edu

References

1 PAULSON, M., KUNDUKULAM, S.O., AANANDAN, C.K., and MOHANAN, P.: 'A new compact dual-band dual-polarized microstrip antenna', *Microw. Opt. Technol. Lett.*, 2001, **29**, pp. 315–317

2 GEORGE, J., AANANDAN, C.K., MOHANAN, P., and NAIR, K.G.: 'Analysis of a new compact microstrip antenna', *IEEE Trans.*, 1998, **AP-46**, pp. 1712–1717

3 GEORGE, J., DEEPUKUMAR, M., AANANDAN, C.K., MOHANAN, P., and NAIR, K.G.: 'New compact microstrip antenna', *Electron. Lett.*, 1996, **32**, pp. 508–509

4 DEEPUKUMAR, M., GEORGE, J., AANANDAN, C.K., MOHANAN, P., and NAIR, K.G.: 'Broadband dual frequency microstrip antenna', *Electron. Lett.*, 1996, **32**, pp. 1531–1532

Simple low-cost planar antenna for indoor communication under the Bluetooth protocol

G. Vermeeren, H. Rogier, F. Olyslager and D. De Zutter

A single-feed rectangular-ring microstrip antenna is proposed for indoor communication under the Bluetooth protocol. The dimensions of the antenna together with the location of the feed point are optimised through field simulations in order to cover the Bluetooth bandwidth and to avoid linear polarisation. The performance and the efficiency of the antenna are illustrated in a real indoor environment.

Antenna geometry and design: The introduction of new wireless protocols for indoor communication such as Bluetooth [1], IEEE 802.11 and HiperLAN present real challenges to antenna design. In addition to the performance issue, one of the main concerns for the deployment of Bluetooth products is the cost of the system. In this respect, the availability of a simple and low-cost antenna is a very important feature of a Bluetooth interface. Single-feed planar antennas [2 – 4] offer attractive solutions that can be easily integrated into a Bluetooth system. However, it is well known that microstrip antennas can have a rather narrow bandwidth and low efficiency. Moreover, single-feed solutions are often linearly polarised, making the antenna very polarisation-sensitive. In Fig. 1, we propose a single-feed rectangular-ring microstrip antenna for operation under the Bluetooth protocol. The dimensions of the antenna are specified in Table 1. The structure is implemented on a standard Rogers RT/5870 Duroid substrate, the thickness and permittivity of which were chosen in order to optimise the antenna efficiency. A 50 Ω coaxial feed is used to excite the antenna. In order to obtain a –10 dB return loss in the Bluetooth (ISM) band (2.4–2.483 GHz) and in order to avoid linear polarisation, the geometry of the antenna patch and the location of the feed-point were carefully optimised. Several designs were evaluated with the commercial field simulator Momentum from Agilent Technologies. Linear polarisation is avoided by placing the feed point on a diagonal of the patch, so that two orthogonally polarised modes, TM01 and TM10, are excited. The bandwidth of the design increases by choosing slightly different values for the patch length L and width W and by making a suitable choice of the slot parameters l and w, so that the TM01 and TM10 modes resonate at different frequencies. Increasing the parameter l, for example, results in a lower resonance frequency for the TM01 mode. Once the simulations gave a suitable design, a prototype was built and measured.

Simulation and measurement results: In Fig. 2 the simulation results for the return loss are compared with measurements. As seen, there is excellent agreement between the simulation data, obtained using Momentum, and the measured data. The measured bandwidth of the antenna equals 108 MHz, which is sufficient to cover the Bluetooth band. Fig. 3 shows the radiation patterns in the xz- and yz-planes for the RHCP and LHCP field components at 2.44 GHz. The polarisation of the antenna is nearly circular, assuring good reception for all kinds of transmitter-receiver orientations. Furthermore, the antenna has a high efficiency ($\eta_{simulated}$ = 84%) and the simulated antenna gain equals 6.54 dB.

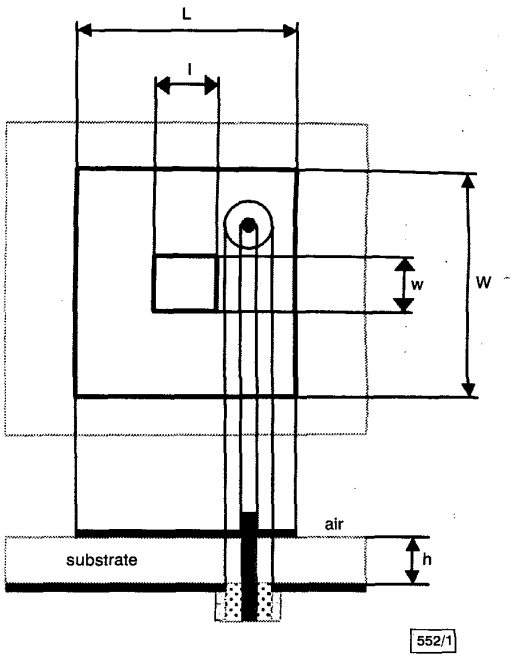

Fig. 1 *Geometry of rectangular-ring microstrip antenna*

Table 1: Dimensions of the rectangular-ring antenna for Bluetooth

Patch		Substrate	
L mm	38.6	h mm	1.5748
W mm	37	ε_r	2.35
Feed point mm	(5.3, 5.3)	tan δ	0.0012
Slot			
l mm	6.4		
w mm	15.6		

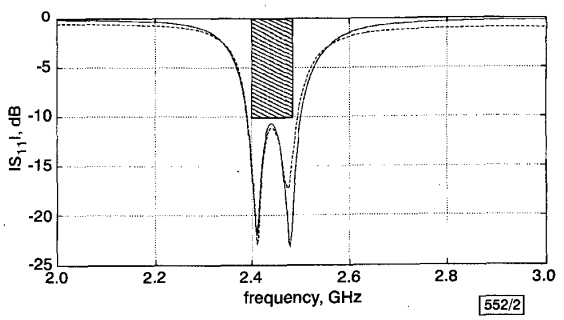

Fig. 2 *Measured and simulated return loss (S_{11}) of rectangular-ring microstrip*

——— measurement
– – – – simulation

To obtain an estimate of the average signal levels in a complex indoor environment, we tested the transmission characteristics of a receiver-transmitter pair in a real indoor environment, shown in Fig. 4. We considered both a line-of-sight (TX1-RX) and a non-line-of-sight (TX2-RX) transmission, with the antenna axes oriented either parallel or perpendicular to each other. In Fig. 4, we have shown the walls and two metallic objects that influence the signal propagation. Smaller furniture is not shown. Both transmitter and receiver antennas are placed vertically 90 cm above the ground. In Fig. 4 the average received power levels when the transmitter emits a 0 dBm continuous wave signal are presented, for the two transmitter-receiver pairs and for both orientations. For the line-of-sight situation, the in-band reception is better than –40 dBm for an antenna separation of 156 cm in both orientations. For the non-line-of-sight case, reception is clearly worse, with all kinds of obstacles blocking the propagation path. Yet signals